Table S1 Clinical data of all patients (n=11; data obtained from GSE131882, GSE151302, and GSE195460)

Group	CON	DN
Total	6	5
Age (years)	56.333±5.001	62.400±12.700
Gender		
Female	3	2
Male	3	3
A1C	–	8.300±1.594
GFR (mL/min/1.73 m^2)	74.612±15.505	78.972±17.043
Serum creatinine	1.010±0.225	0.952±0.221
Hypertension	3	2
Glomerulosclerosis		
None	5	1
10–25%	1	2
26–50%	0	2
IFTA		
0%	1	0
1–10%	5	1
11–25%	0	2
26–50%	0	2
Arteriosclerosis	6	5

Data are presented as number or mean ± SD. CON, control; DN, diabetic nephropathy; GFR, glomerular filtration rate; IFTA, interstitial fibrosis and tubular atrophy; SD, standard deviation.

https://dx.doi.org/10.21037/tau-24-569

Table S2 Markers of renal cells

Abbreviations	Cell type	Markers
PT	Proximal tubule	CUBN, HAVCR1, SLC5A1, SLC5A2, VCAM1
PEC	Parietal epithelial cells	CFH
TAL	Thick ascending limb	SLC12A1, CLDN10, CLDN16
DCT1 and DCT2	Distal convoluted tubule 1/2	SLC12A3, TRPM6
DCT2/CNT	Distal convoluted tubule 2/connecting tubule	SCNN1G, TRPV5
CNT	Connecting tubule	CALB1
ICA and ICB	Type A/B intercalated cells	ATP6V0D2, SLC4A1, SLC26A7, SLC26A4
PODO	Podocytes	NPHS1, NPHS2
ENDO	Endothelial cells	PECAM1, FLT1
MES and JGA	Mesangial cells/juxtaglomerular apparatus	ITGA8, PDGFRB, MEIS2, PIEZO2, REN
FIB	Fibroblasts	ACTA2, CALD1
IMC	Iummne cells	PROX1, FLT4, PDPN, PTPRC, CD3E, MS4A1, FCGR3A, CD14, CSF1R

PT, proximal tubule; PEC, parietal epithelial cell; TAL, thick ascending limb; DCT, distal convoluted tubule; CNT, connecting tubule; ICA, type A intercalated cells; ICB, type B intercalated cells; PODO, podocyte; ENDO, endothelial cell; MES, mesangial cells; FIB, fibroblasts; IMC, immune cell.

https://dx.doi.org/10.21037/tau-24-569

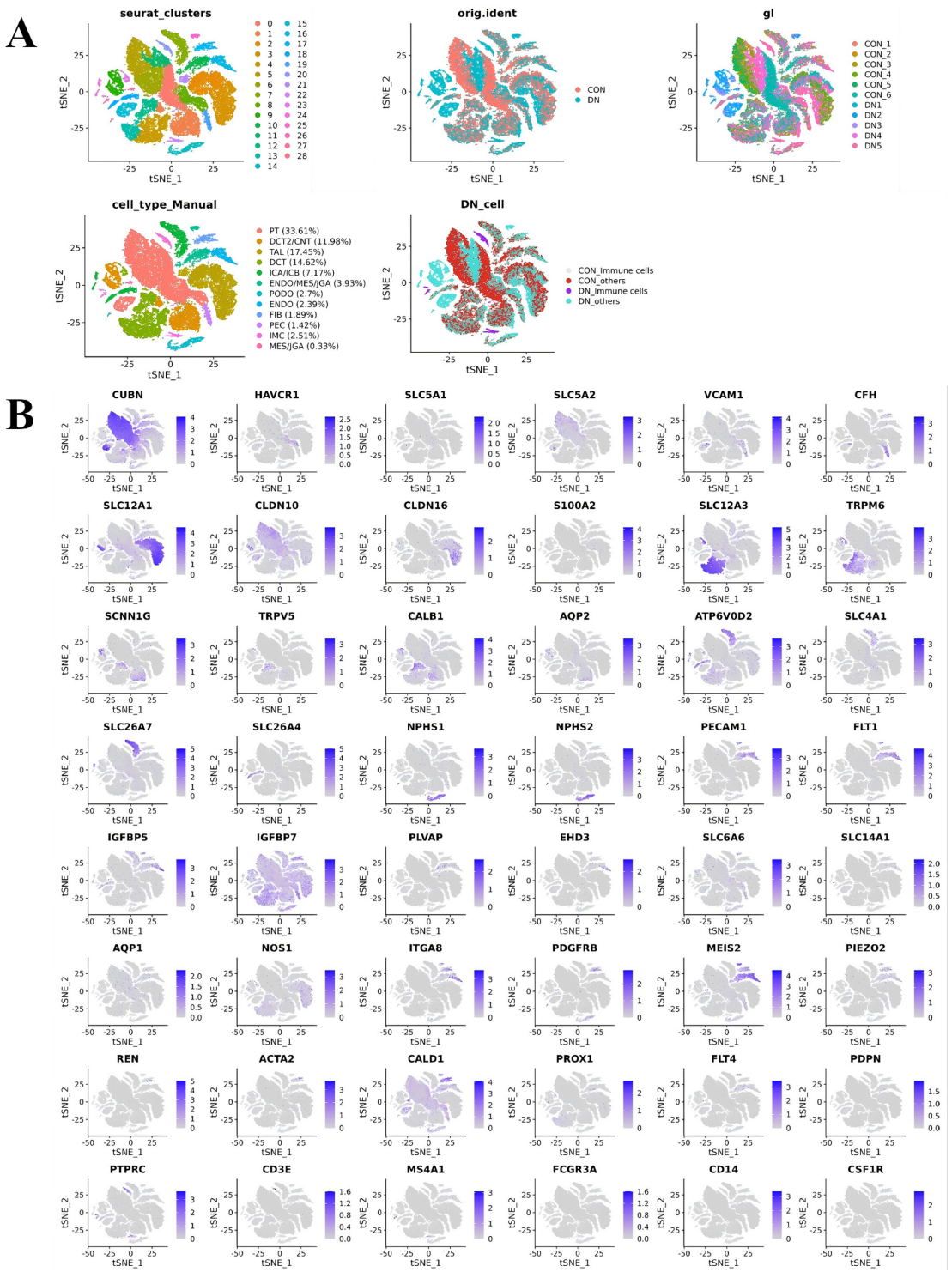

Figure S1 The distribution of tSNE in kidney snRNA-seq. (A) The distribution of tSNE in cell clusters, groups, samples, kidney cell types, and IMCs. (B) The expression and distribution of renal cell markers. tSNE, t-distributed stochastic neighbor embedding; CON, control; DN, diabetic nephropathy; PT, proximal tubule; DCT, distal convoluted tubule; CNT, connecting tubule; TAL, thick ascending limb; ICA, type A intercalated cells; ICB; type B intercalated cells; ENDO, endothelial cell; MES, mesangial cells; JGA, juxtaglomerular apparatus; PODO, podocytes; FIB, fibroblasts; PEC, parietal epithelial cell; IMC, immune cell; snRNA-seq, single-nuclear RNA sequencing.

https://dx.doi.org/10.21037/tau-24-569

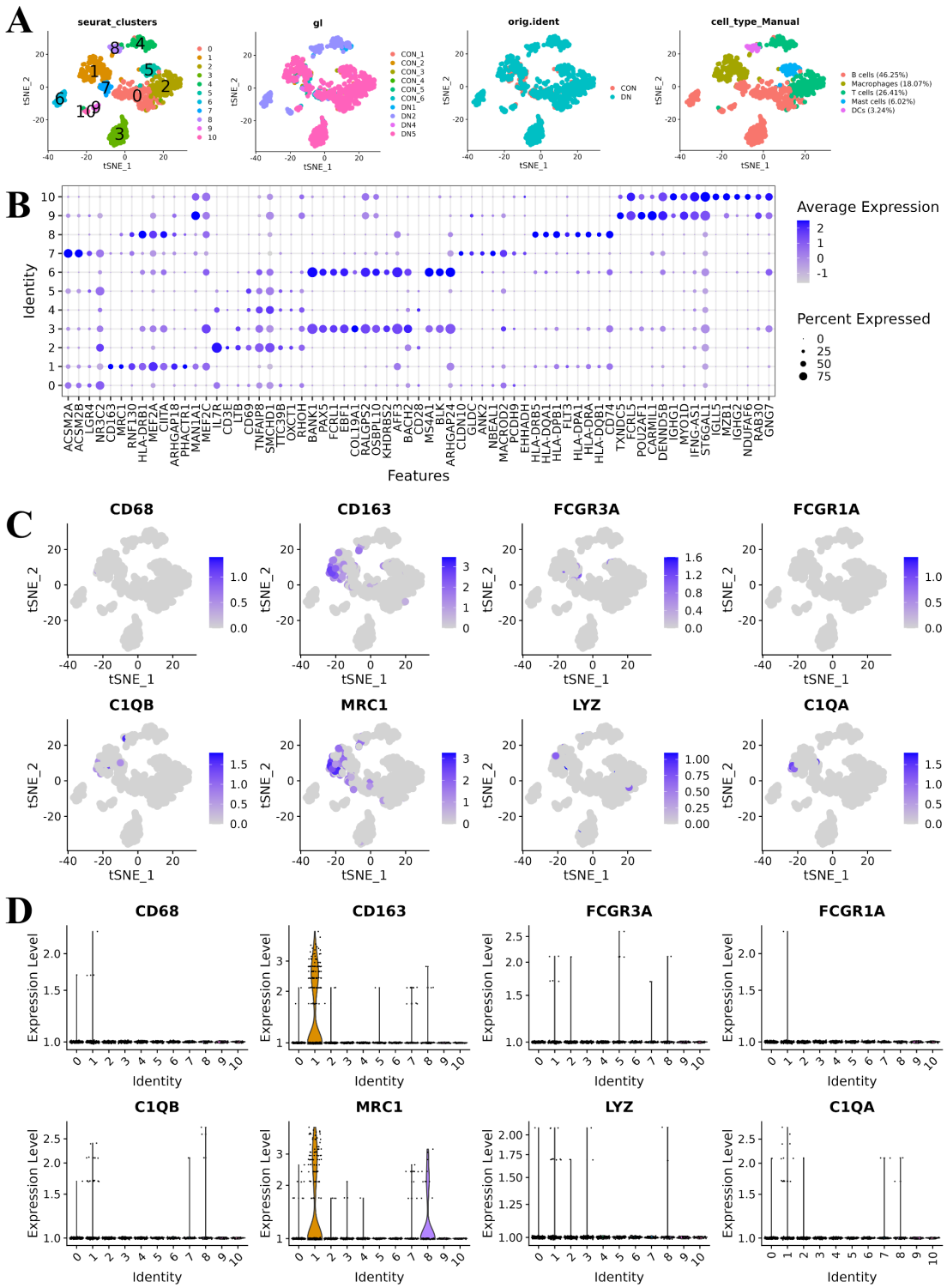

Figure S2 Dimension reduction distribution results of immune-cell tSNE. (A) The distribution of tSNE in different cell clusters, groups, samples, and cell types of IMCs. (B) The expression of markers in different cell clusters of IMCs. (C) The distribution of tSNE expressed by the Mφs' markers. (D) Violin plot showing the expression level of Mφs' markers in different cell clusters. tSNE, t-distributed stochastic neighbor embedding; CON, control; DN, diabetic nephropathy; DCs, dendritic cells; IMC, immune cell; Mφ, macrophage.

https://dx.doi.org/10.21037/tau-24-569

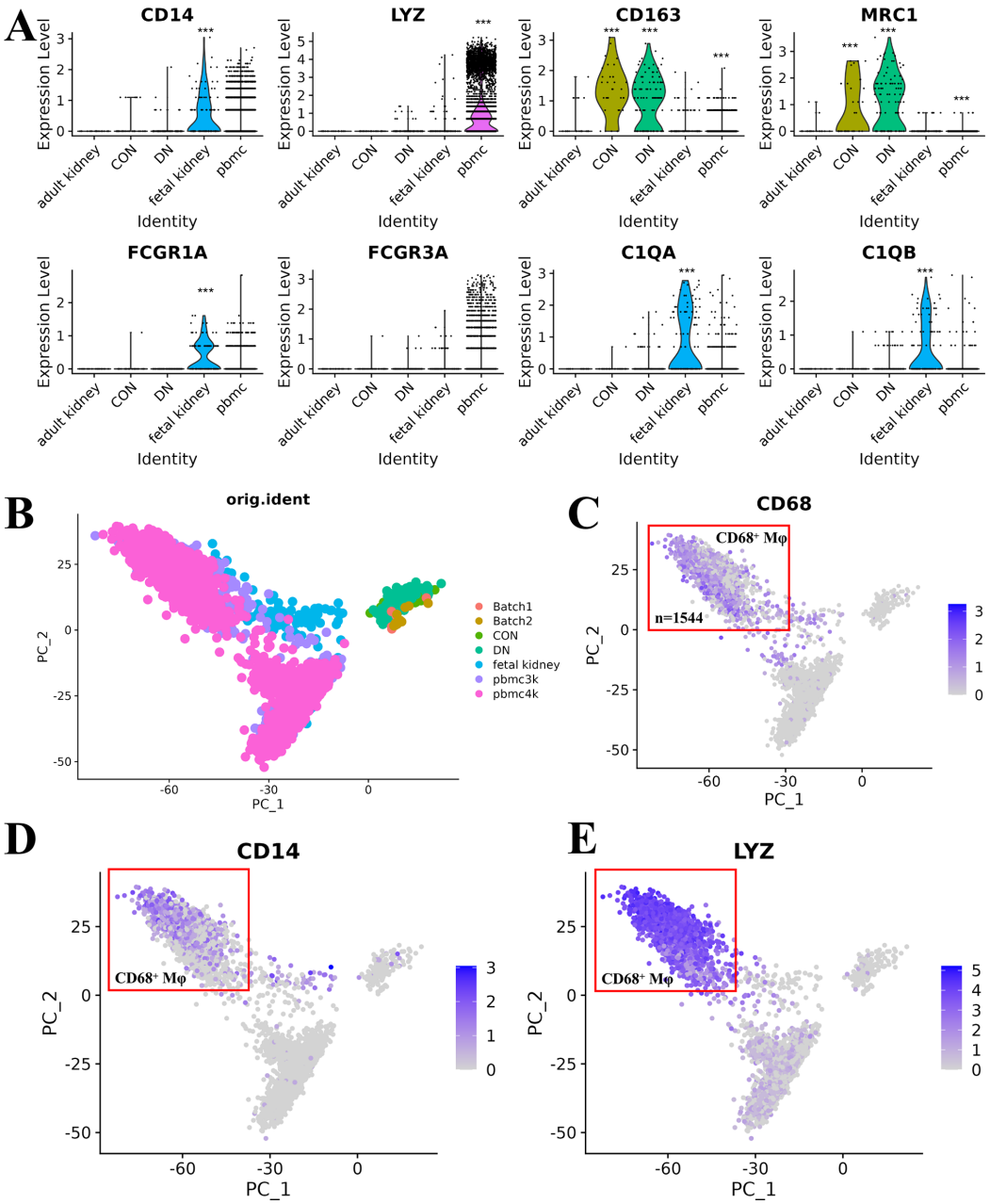

Figure S3 Expression of markers of resident KRMs in various types of tissues. (A) The expression levels of CD14 and seven key markers. Compared to other types of cells, CD163, MRC1, and LYZ were significantly differently expressed in PBMCs. (B) The distribution of PC1 and PC2 in each tissue after dimensionality reduction. The distribution of PBMCs overlapped with that of IMCs in fetal kidney and was different from that of KRMs. (C-E) The expression density of CD68, CD14, and LYZ. CD68 was used to label PBMCs as blood Mφs, which was mutually verified with $CD14^+$ Mφs. $CD14^+$ Mφs and $CD68^+$ Mφs overlapped in distribution and expression with LYZ. Adult kidneys, also labelled as batch1 and batch2, were sourced from GSE118184 and GSE114156. Fetal kidney was an IMC derived from GSE112570. PBMCs, also labelled with PBMC3K and PBMC4K, were downloaded using TENxPBMCData v. 1.14.0. CON and DN group Mφs were obtained from GSE131882, GSE151302, and GSE195460. ***, indicate P<0.001 *vs.* CON group. Red squares emphasize the highly expressed CD68 Mφs cluster (C), as well as the $CD68^+$ Mφs cluster rich in CD14 (D) and LYZ (E) expression. CON, control; DN, diabetic nephropathy; PC, principal component; KRM, kidney resident Mφ; Mφ, macrophage; PBMC, peripheral blood mononuclear cell; IMC, immune cell.

https://dx.doi.org/10.21037/tau-24-569

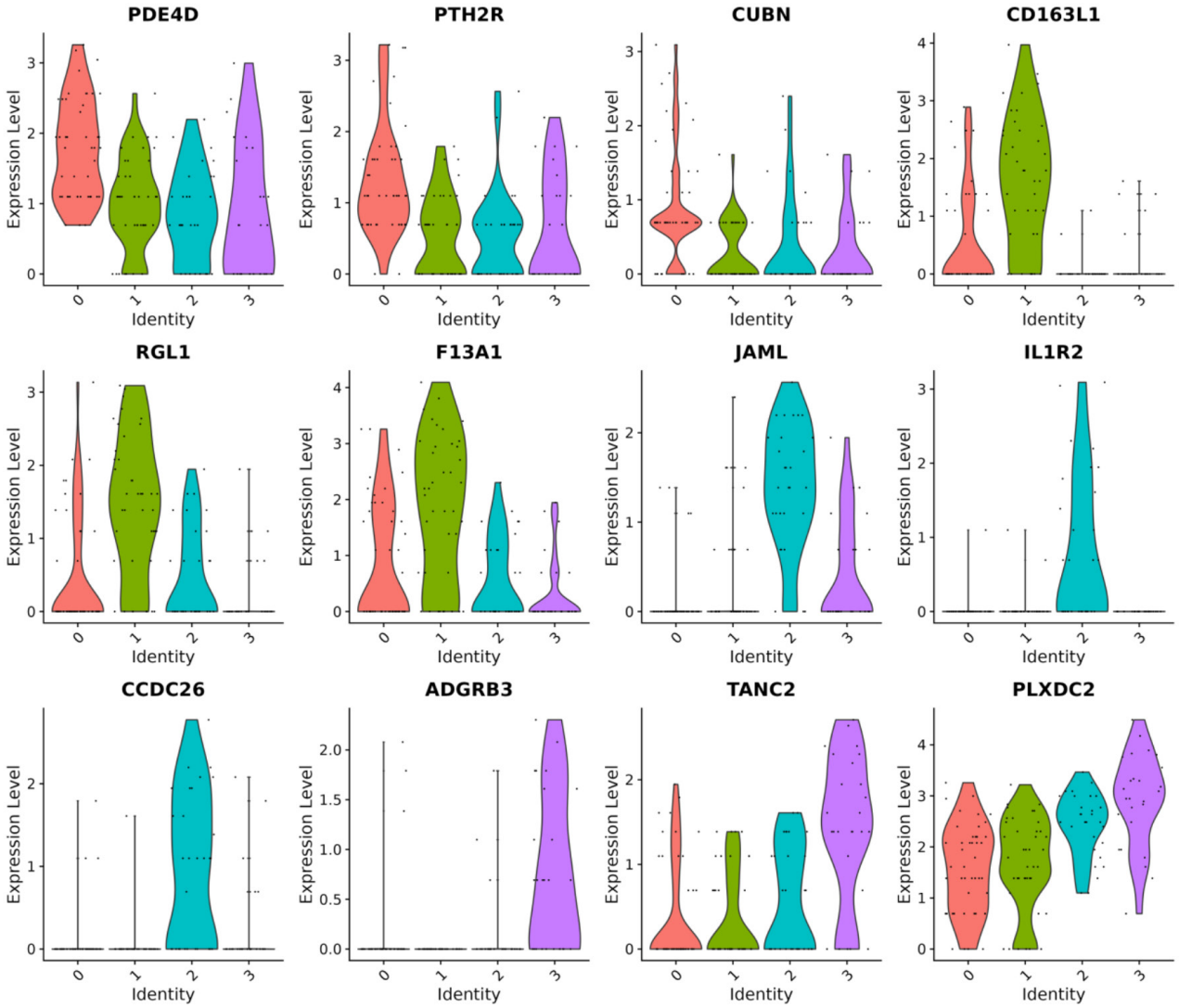

Figure S4 Expression of the top 3 markers in different Mφ subtypes. Mφ, macrophage.

https://dx.doi.org/10.21037/tau-24-569

Table S3 Interaction intensity between KRMs and renal cells (celltalker; P<0.05)

Cell type 1	Cell type 2	Interact ratio
PODO	Mφs	37.39928
Mφs	ENDO	29.83614
Mφs	B cells	28.28833
PODO	Mφs	26.60931
Mφs	ENDO	26.0684
ENDO/MES/JGA	Mφs	18.94795
DCT	Mφs	17.10896
PEC	Mφs	14.88684
FIB	Mφs	14.46386
Mφs	ENDO	13.98918
FIB	Mφs	13.94389
TAL	Mφs	13.77417
MES/JGA	Mφs	13.67703
PT	Mφs	13.62664
B cells	Mφs	13.48324
PODO	Mφs	12.71048
Mφs	PODO	12.29298
ICA/ICB	Mφs	11.90628
DCT	Mφs	11.89316
PODO	Mφs	11.6114

KRM, kidney resident Mφ; Mφ, macrophage; PODO, podocyte; ENDO, endothelial cell; MES, mesangial cells; JGA, juxtaglomerular apparatus; DCT, distal convoluted tubule; PEC, parietal epithelial cell; FIB, fibroblasts; TAL, thick ascending limb; MES, mesangial cells; PT, proximal tubule.

https://dx.doi.org/10.21037/tau-24-569

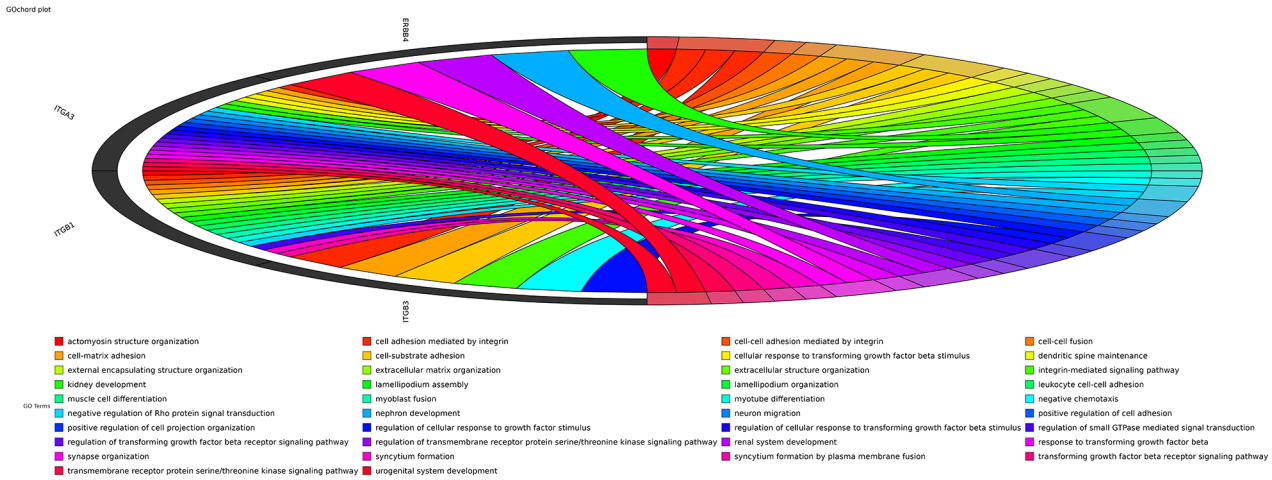

Figure S5 BPs in which the key receptors of PODOs participate. BP, biological process; PODO, podocyte.

https://dx.doi.org/10.21037/tau-24-569